Contribution from the Departament de Quimica Inorgânica, Universitat de Valencia, Burjassot, Valencia, Spain, and Laboratoire de Chimie de Coordination du CNRS, Toulouse, France

Extremely Weak Magnetic Exchange Interactions in terpy-Containing Copper(II) Dimers. Crystal and Molecular Structure of Cu(terpy)(CA)·H_2O and $[Cu_2(terpy)_2(CA)](PF_6)_2$ Complexes (terpy = 2,2′:6′,2″-Terpyridine, CA = Dianion of Chloranilic Acid)

José V. Folgado,† Rafael Ibáñez,† Eugenio Coronado,† Daniel Beltrán,*† Jean M. Savariault,‡ and Jean Galy‡

Received June 10, 1987

Four new copper(II) complexes containing 2,2′:6′,2″-terpyridine (terpy) and the dianions of chloranilic (CA) or oxalic (OX) acids have been prepared. The X-ray crystal structures of Cu(terpy)(CA)·H_2O (I) and $[Cu_2(terpy)_2(CA)](PF_6)_2$ (III) are presented. Complex I, $C_{21}H_{13}O_5Cl_2CuN_3$, is monoclinic, with space group $C2/c$ and lattice parameters a = 22.19 (2) Å, b = 13.614 (5) Å, c = 15.32 (1) Å, β = 119.71 (3)°, V = 4019.7 Å^3, and Z = 8. Complexes II, $C_{36}H_{22}O_{12}Cl_4Cu_2N_6$, and III, $C_{36}H_{22}O_4Cl_2P_2F_{12}Cu_2N_6$, are isostructural, monoclinic, with space group $P2_1/n$ and lattice parameters a = 9.002 (1)/9.217 (5) Å, b = 12.597 (2)/12.852 (2) Å, c = 16.538 (3)/16.642 (9) Å, β = 102.63 (1)/101.61 (2)°, V = 1830/1931 Å^3, and Z = 2, respectively. Complex I is associated in pseudodimeric entities formed by two Cu(terpy)(CA)·H_2O moieties connected via hydrogen bonding whereas the structure of III is built up by dimeric $[Cu_2(terpy)_2(CA)]^{2+}$ cations and PF_6^- anions. The copper(II) ion coordination geometry is five-coordinate and intermediate between trigonal bipyramidal and square pyramidal in I and close to square pyramidal in III. From variable-temperature magnetic susceptibility measurements (4.2–300 K) weak antiferromagnetic exchange interactions ($2J$ = −1.6 cm^{-1}) are seen for the $[Cu_2(terpy)_2(OX)](PF_6)_2$ complex (IV) whereas no exchange interactions are detected for the other complexes (I–III). Room-temperature EPR spectra of all the studied complexes show the $\Delta M_s = \pm 2$ forbidden transition. The observation of temperature-dependent singlet-to-triplet forbidden EPR transitions (in the 100–500 K range) in the CA complexes allows one to determine the exchange parameters (between 0.04 and 0.12 cm^{-1}) as well as the thermal evolution. The observed exchange interactions are discussed on the basis of the structural findings. In particular, a discussion about the feasible paths of exchange interactions in compound I is presented.

Introduction

The study of exchange-coupled polynuclear complexes is an active area of coordination chemistry. In particular, significant progress has been made in the understanding of the exchange interaction phenomenon.[1] In general, a close dependence of the isotropic exchange parameter J on some structural factors has been demonstrated and understood on the basis of the orbital mechanism of the exchange interaction.[2]

In most of the polynuclear complexes reported so far, the experimental magnetic behavior vs temperature has been explained in reasonable agreement with theory by assuming a unique value of J. Thus, for the analysis of the magnetic properties of copper dimers the so-called Bleaney–Bowers formula has been assumed currently. In some cases, however, a temperature-dependent value of J has been further invoked in order to explain the experimental behavior of the susceptibility.[3,4] Nevertheless, this is very difficult to demonstrate by the usual magnetochemical procedure because other factors such as a biquadratic exchange term[5] or an anisotropic exchange[6] have a similar effect on the susceptibility. Spectroscopic techniques, such as optical spectroscopy,[7] inelastic neutron scattering,[8] or EPR,[9,10] have been shown to be very useful as complements to the magnetochemical measurements because they offer more direct access to the singlet–triplet energy gap. The range of exchange energies detectable by EPR is restricted by the microwave radiation used ($2|J| < 0.3$ cm^{-1} for X-band).

Our current interest in this area is focused on the design of new polymetallic complexes of copper(II) exhibiting very weak J values, since in such situations small structural changes could entail a reversal in the sign of J. In this context we have reported the synthesis and magnetic characterization of a wide set of pentacoordinated copper(II) compounds containing the entity [Cu(L_{III})X], where L_{III} is a tridentate rigid "quasi-planar" ligand such as terpy (2,2′:6′,2″-terpyridine), paphy (pyridine-2-carboxaldehyde 2-pyridylhydrazone), TPT (2,4,6-tris(2-pyridyl)-1,3,5-triazine) or BPCA (*N*-(2-pyridinylcarbonyl)-2-pyridinecarboximidate anion) and X a halide or pseudohalide anion.[11–17]

Planarity of these ligands favors the stacking of square-parallel [Cu(L_{III})X] moieties bridged by the X^- anions to give dimers or more extended magnetic systems (linear or ladderlike chains). In general, due to the poor effective overlap between the magnetic orbitals determined by this geometry, very weak antiferromagnetic J values (around 1–3 cm^{-1}) have been observed.[12–14]

In this work we have synthesized and characterized four new terpy-containing copper(II) complexes using as bridging ligands the dianions of chloranilic (CA) and oxalic (OX) acids, which have a proven ability for acting as bridges in this kind of geometry.[18] The change of the (pseudo)halogen by multiatom bridges has led to dimers with larger intramolecular metal–metal distances and, consequently, with weaker exchange interactions. Thus, the extremely weak exchange interactions of the CA complexes have allowed the observation of singlet-to-triplet transitions in the EPR spectra.

Experimental Section

Compound Preparation. Cu(terpy)(CA)·H_2O (I) was prepared by the

(1) Willett, R. D., Gatteschi, D., Kahn, O., Eds. *Magneto-structural Correlations in Exchange-Coupled Systems*; NATO ASI Series; Reidel: Dordrecht, Holland, 1985.
(2) Kahn, O. *Angew. Chem., Int. Ed. Engl.* **1985**, *24*, 834.
(3) Mikuriya, M.; Okawa, H.; Kida, S. *Bull. Chem. Soc. Jpn.* **1981**, *54*, 2979.
(4) Kahn, O.; Morgenstern-Badarau, I.; Audiere, P.; Lehn, J. M.; Sullivan, S. A. *J. Am. Chem. Soc.* **1980**, *102*, 5935.
(5) Lines, M. E. *Solid State Commun.* **1972**, *11*, 1615.
(6) Nakatsuka, S.; Osaki, K.; Uryu, N. *Inorg. Chem.* **1982**, *21*, 4332.
(7) See e.g.: Gudel, H. U. In ref 1, p 297, and references therein.
(8) See e.g.: Gudel, H. U. In ref 1, p 329, and references therein.
(9) Pierpont, C. G.; Francesconi, L. C.; Hendrickson, D. N. *Inorg. Chem.* **1977**, *16*, 2367.
(10) Duggan, D. M.; Hendrickson, D. N. *Inorg. Chem.* **1974**, *13*, 2929.
(11) Rojo, T.; Darriet, J.; Dance, J. M.; Beltran, D. *Inorg. Chim. Acta* **1982**, *64*, L105.
(12) Folgado, J. V.; Coronado, E.; Beltran, D. *J. Chem. Soc., Dalton Trans.* **1986**, 1661.
(13) Coronado, E.; Drillon, M.; Beltran, D. *Inorg. Chim. Acta* **1984**, *82*, 13.
(14) Rojo, T.; Darriet, J.; Villeneuve, G.; Arriortua, M. I.; Ruiz, J.; Beltran, D. *J. Chem. Soc., Dalton Trans.* **1987**, 285.
(15) Folgado, J. V.; Escriva, E.; Beltran-Porter, A.; Beltran-Porter, D. *Transition Met. Chem. (Weinheim, Ger.)* **1986**, *11*, 485.
(16) Folgado, J. V.; Escriva, E.; Beltran-Porter, A.; Beltran-Porter, D. *Transition Met. Chem. (Weinheim, Ger.)*, in press.
(17) Folgado, J. V.; Escriva, E.; Beltran-Porter, A.; Beltran-Porter, D.; Fuertes, A.; Miravitlles, C. *Polyhedron* **1987**, *6*, 1533.
(18) Felthouse, T. R.; Laskowski, E. J.; Hendrickson, D. N. *Inorg. Chem.* **1977**, *16*, 1077.

†Universitat de Valencia.
‡Laboratoire de Chimie de Coordination du CNRS.

0020-1669/88/1327-0019$01.50/0

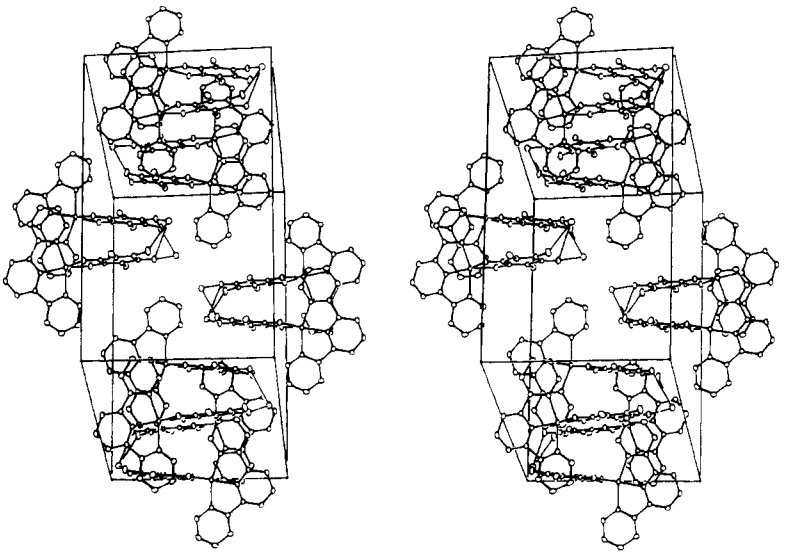

Figure 1. Stereoscopic view of the cell of complex I. The hydrogen atoms have been omitted for clarity.

following procedure: A 0.085-g (0.5-mmol) amount of $CuCl_2 \cdot 2H_2O$ in 20 mL of warm water was mixed, with stirring and heating, with 0.117 g (0.5 mmol) of terpy in 15 mL of warm acetone. To the resulting green solution was slowly added with stirring 0.104 g (0.5 mmol) of chloranilic acid in 75 mL of warm water, to give a purple precipitate. The crystalline powder was vacuum-filtered, washed several times with cold water and acetone, followed by several washings with anhydrous ethyl ether, and stored over silica gel. The solid is very poorly soluble in common solvents, but it is possible to obtain suitable crystals for X-ray studies from extremely dilute aqueous solutions at pH 11. Anal. Found (calcd) for $C_{21}H_{13}O_5Cl_2CuN_3$: Cu, 12.2 (12.2); C, 48.4 (48.3); N, 8.1 (8.1); H, 2.4 (2.5).

$[Cu_2(terpy)_2(CA)](ClO_4)_2$ (II) was obtained by two different methods: (A) A 0.296-g (0.8-mmol) amount of $Cu(ClO_4)_2 \cdot 6H_2O$ in 25 mL of warm water was mixed, with stirring and heating, with 0.187 g (0.8 mmol) of terpy in 15 mL of warm acetone. To the resulting solution was slowly added 0.084 g (0.4 mmol) of chloranilic acid in 50 mL of warm water, to give a blue-grey precipitate, which was vacuum-filtered, washed, dried, and stored as above. (B) Warm solutions containing $CuCl_2 \cdot 2H_2O$ (0.8 mmol in 50 mL of water) and terpy (0.8 mmol in 15 mL of acetone) were mixed with stirring. Acetone was removed by heating, and the solution was adjusted to pH 8. Then, a basic warm aqueous solution (50 mL, pH 11) containing 0.4 mmol of chloranilic acid was added with stirring and heating (80 °C). The resulting purple-blue solution was filtered through a low-porosity frit, and with stirring and heating, a filtered aqueous solution of $NaClO_4 \cdot H_2O$ was added. By slow evaporation at room temperature dark purple-blue crystals appeared, which were separated by filtration, washed, dried, and stored as above. Anal. Found (calcd) for $C_{36}H_{22}O_{12}Cl_4Cu_2N_6$: Cu, 12.6 (12.7); C, 43.3 (43.2); N, 8.5 (8.4); H, 2.2 (2.2).

Crystals of $[Cu_2(terpy)_2(CA)](PF_6)_2$ (III) were obtained by method B but with KPF_6 instead of $NaClO_4 \cdot H_2O$. Anal. Found (calcd) for $C_{36}H_{22}O_4Cl_2P_2F_{12}Cu_2N_6$: Cu, 11.7 (11.7); C, 39.4 (39.6); N, 7.8 (7.7), H, 2.0 (2.0).

$[Cu_2(terpy)_2(OX)](PF_6)_2$ (IV) was prepared as for the CA analogue, with $K_2C_2O_4 \cdot H_2O$ substituted for $(CA)H_2$; starting solutions were more concentrated (1 mmol of $CuCl_2 \cdot 2H_2O$ in 15 mL of water, 1 mmol of terpy in 10 mL of acetone, 0.5 mmol of $K_2OX \cdot H_2O$ in 5 mL of water) and were at pH 8. Anal. Found (calcd) for $C_{32}H_{22}O_4P_2F_{12}Cu_2N_6$: Cu, 13.0 (13.1); C, 39.4 (39.5); N, 8.5 (8.7); H, 2.2 (2.3). The title green anhydrous compound was isolated at 80 °C whereas at room temperature a dihydrate compound ($[Cu_2(terpy)_2(OX)](PF_6)_2 \cdot 2H_2O$) resulted.

Physical Measurements. Infrared spectra were obtained on KBr pellets in the 4000–250-cm^{-1} region with a Pye Unicam SP 2000 spectrophotometer. Diffuse-reflectance electronic spectra were recorded on a Perkin-Elmer Lambda 9 UV/vis/near-IR spectrophotometer. Magnetic measurements were performed in the temperature range 4–298 K with a pendulum-type apparatus equipped with a helium cryostat. The uncertainty in the data is lower than 0.1 K for temperatures and 2×10^{-5} cm^3 mol^{-1} for susceptibilities. Experimental susceptibilities were corrected for the diamagnetic contributions and for the TIP, estimated to be 60×10^{-6} cm^3 mol^{-1} per Cu(II) ion. EPR spectra were recorded on a Bruker ER 200D spectrometer equipped with a nitrogen cryostat.

X-ray and Structure Determination. Crystal data and space groups of the compounds I–III were determined by using photographic methods. The cell dimensions were refined from the setting angles of 25 reflections of crystals mounted at room temperature on an Enraf-Nonius CAD4 automatic diffractometer with Mo Kα monochromated radiation. Crystals of II and III being isostructural, the structure determination of III was preferred because of the quality of the crystals. The three compounds crystallize as dark purple blocks having a parallelepipedic shape. Physical properties and parameters pertinent to data collection, structure solution, and refinement are reported in Table I. After absorption correction, the measured symmetric equivalent reflections were averaged. Patterson synthesis gave the starting point for the structure, which was then progressively determined by subsequent difference Fourier syntheses and least-squares refinements. Anisotropic thermal parameters were introduced for all atoms except for hydrogen atoms, which were refined with isotropic thermal parameters. The PF_6 group in compound III was found with a disorder in the positions of some fluorine atoms with the F(3)–F(4) direction as an eightfold axis.

Scattering factors and anomalous dispersion coefficients were taken from ref 19. All calculations were performed by using the Enraf-Nonius Structure Determination Package including ORTEP for drawings.[20] The final atomic and equivalent isotropic thermal factors are reported in Table II.

Results and Discussion

Structure of I. Figure 1 shows a stereoscopic view of the cell contents. The compound is associated in pseudodimeric entities formed by two $Cu(terpy)(CA) \cdot H_2O$ moieties connected via hydrogen bonding. Each water molecule is bonded to two terminal oxygen atoms from different CA anions; i.e., O(w) links together O(4) and O′(3).

A general view of the monomeric moiety is represented in Figure 2 with an additional drawing of the hydrogen-bonding system. The copper(II) atom is five-coordinated to the three nitrogen atoms from terpy and two oxygen atoms from CA. The ligand to metal bond distances are roughly 2 Å. The mean planes of the terpy and CA ligands are nearly orthogonal (90.2 (4)°). In the "dimeric" entities the planes of the terpy ligands are parallel with an interval of 3.63 (4) Å while the planes of CA groups make an angle of 11.4 (6)°. This fact leads to an offset between the two terpy ligands in such a way that the pairs N(1), C(5) and N′(1), C′(5) are one above the other. On the other hand, the plane defined by the atoms Cu, O(1), and O(2) makes an angle of 6.5 (4)° with the CA plane. The resulting "intradimer" Cu–Cu distance is then equal to 5.648 (1) Å, whereas the nearest "interdimeric" distance is somewhat longer (5.735 (1) Å).

Structure of III. The structure of III consists of layers, parallel to the (100) plane, built up by dimeric $[Cu_2(terpy)_2(CA)]^{2+}$

(19) Cromer, D. T.; Waber, J. T. *International Tables for X-ray Crystallography*; Kynoch: Birmingham, England, 1974; Vol. IV, pp 72–98.
(20) Frenz, B. A. *The Enraf-Nonius CAD4 SDP*; Schent, H., Olthof-Hazelkamp, R., van Konisgsveld, H., Bassi, G. G., Eds.; Delft University Press: Delft, Holland, 1978.

Table I. Physical Properties and Parameters of Data Collection and Refinement

Physical Properties

	I	III	II
formula	$CuCl_2O_5N_3C_{21}H_{13}$	$Cu_2Cl_2P_2F_{12}O_4N_6C_{36}H_{22}$	$Cu_2Cl_4O_{12}N_6C_{36}H_{22}$
mol wt, g	521.8	1090.5	999.5
cryst syst	monoclinic	monoclinic	monoclinic
space group	$C2/c$	$P2_1/n$	$P2_1/n$
a, Å	22.19 (2)	9.217 (5)	9.002 (1)
b, Å	13.614 (5)	12.852 (2)	12.597 (2)
c, Å	15.32 (1)	16.642 (9)	16.538 (3)
β, deg	119.71 (8)	101.61 (2)	102.63 (1)
V, Å^3	4019.7 (8)	1931 (2)	1830 (1)
Z	8	2	2
d_{calcd}, g/cm^3	1.72	1.87	1.81
d_{measd}, g/cm^3	1.69 (5)	1.85 (6)	1.79 (7)
$F(000)$	2104	1084	
cryst shape			
faces	{10$\bar{1}$}, {110}, {$\bar{1}$10}	{012}, {1$\bar{1}$0}, {1$\bar{1}$0}	
dist, cm	0.030, 0.009, 0.010	0.020, 0.010, 0.017	

Parameters of Data Collection and Refinement

	I	III
	Measurements	
λ, Å	0.7107	0.7107
takeoff angle, deg	3.00	3.25
detector width, mm	4 × 4	4 × 4
scan type	$\omega/2\theta$	$\omega/2\theta$
scan width, deg	0.90 + 0.35 tan θ	0.92 + 0.35 tan θ
θ range, deg	1–32.5	1–32.5
no. of measd rflcns	7416	7604
stds (period.)		
intens (1 h)	{008}, {17$\bar{1}$}, {027}	{$\bar{4}$6$\bar{1}$}, {281}, {$\bar{6}$04}
orientation (100 rflcns)	{10,0,0}, {00$\bar{8}$}, {84$\bar{2}$}	{1,4,1$\bar{1}$}, {$\bar{5}$65}, {4$\bar{6}$0}
abs cor		
μ(Mo Kα), cm^{-1}	13.96	14.32
Gaussian grid	6 × 4 × 12	6 × 8 × 8
transmission factor	0.84–0.91	0.83–0.89
	Refinements	
no. of variables, NV	341	332
no. of unique rflcns with $I > 3\sigma$, NO	3234	3209
weighting scheme	$w = 1/[\sigma^2(I) + (0.6I)^2]^{1/2}$	$w = 1$
highest peak in last diff Fourier, e/Å^3	0.36	0.57
agreement factors		
$R = (\sum\|\|F_o\| - \|F_c\|\|)/(\sum\|F_o\|)$	0.037	0.054
$R_w = [\sum w(\|F_o\| - \|F_c\|)^2/\sum w\|F_o\|^2]^{1/2}$	0.046	0.055
$s = [\sum w(\|F_o\| - \|F_c\|)^2/(NO - NV)]^{1/2}$	1.09	1.80

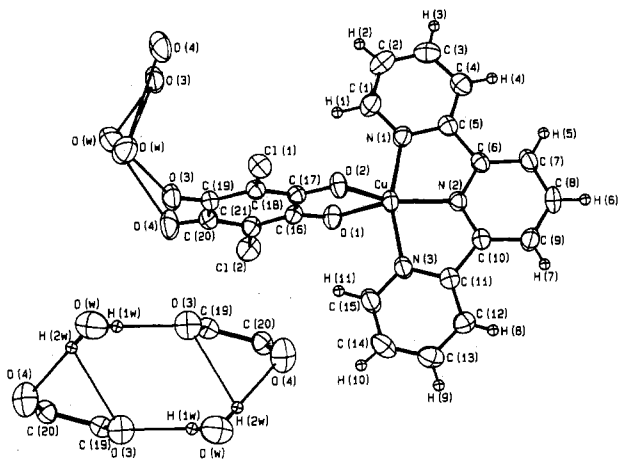

Figure 2. Perspective view of complex I with labeling of atoms and a detailed drawing of the hydrogen bridge network. Thermal ellipsoids are drawn at the 50% probability level for the non-hydrogen atoms and with an arbitrary radius for the hydrogen atoms.

entities and PF_6^- ions. Two crystallographically equivalent layers are interspaced with a similar layer offset by half the cell, whose elements are deduced from the ones of the former layers by an inversion center. The CA groups are twisted by an angle of 17.3 (5)° to the (010) plane and terpy groups by an angle of 36.2 (4)° to the (100) plane. Figure 3 shows a perspective view of the cation with the detailed labeling of the atoms. Similarly to complex I, each copper(II) ion is coordinated to the three nitrogen atoms from terpy and two oxygen atoms from the CA ligand that acts in this case in a bridging bis-bidentate fashion. The intramolecular Cu–Cu distance is equal to 7.843 (1) Å, and the shortest intermolecular one is 7.947 (1) Å. The CA ligand is situated in a plane nearly orthogonal to that of terpy (83.5 (4)°).

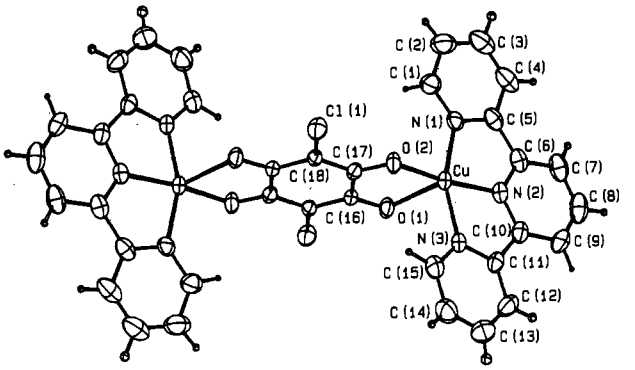

Figure 3. Perspective view of the $[Cu_2(terpy)_2(CA)]^{2+}$ cation in III with atoms labeled. Thermal ellipsoids are as in Figure 2.

Comparison between the Molecular Structures of Compounds I and III. In Table III, the main interatomic distances and angles

Table II. Atomic Parameters and Equivalent Isotropic Thermal Parameters with Their Estimated Standard Deviations[a]

atom	x/a	y/b	z/c	U_{eq}, Å^2	atom	x/a	y/b	z/c	U_{eq}, Å^2
				Cu(terpy)(CA)·H_2O					
Cu	0.35524 (2)	0.89111 (3)	0.61771 (3)	0.0359 (1)	C(13)	0.1425 (2)	0.8716 (3)	0.6236 (2)	0.044 (1)
N(1)	0.4399 (1)	0.8398 (2)	0.6158 (2)	0.0357 (7)	C(14)	0.1646 (2)	0.9623 (3)	0.6134 (2)	0.0491 (9)
N(2)	0.3433 (1)	0.7518 (2)	0.6278 (2)	0.0299 (6)	C(15)	0.2259 (2)	0.9702 (3)	0.6120 (3)	0.0470 (7)
N(3)	0.2648 (1)	0.8917 (2)	0.6204 (2)	0.0372 (7)	O(1)	0.3309 (1)	1.0040 (2)	0.5180 (2)	0.0374 (6)
C(1)	0.4884 (2)	0.8924 (3)	0.6096 (2)	0.044 (1)	O(2)	0.4003 (1)	1.0065 (2)	0.7152 (1)	0.0370 (6)
C(2)	0.5430 (2)	0.8498 (3)	0.6052 (3)	0.048 (1)	O(3)	0.4162 (1)	1.3501 (2)	0.7131 (2)	0.0467 (7)
C(3)	0.5479 (2)	0.7503 (3)	0.6060 (2)	0.047 (1)	O(4)	0.3522 (2)	1.3460 (2)	0.5123 (2)	0.0567 (8)
C(4)	0.4989 (2)	0.6931 (3)	0.6136 (2)	0.041 (1)	C(16)	0.3482 (1)	1.0887 (2)	0.5581 (2)	0.0285 (7)
C(5)	0.4460 (2)	0.7399 (2)	0.6200 (2)	0.0324 (9)	C(17)	0.3897 (1)	1.0898 (2)	0.6731 (2)	0.0272 (6)
C(6)	0.3912 (2)	0.6896 (2)	0.6306 (2)	0.0310 (8)	C(18)	0.4114 (1)	1.1780 (2)	0.7231 (2)	0.0298 (7)
C(7)	0.3863 (2)	0.5899 (2)	0.6435 (3)	0.040 (1)	C(19)	0.3983 (1)	1.2695 (2)	0.6722 (2)	0.0325 (8)
C(8)	0.3302 (2)	0.5569 (2)	0.6523 (3)	0.045 (1)	C(20)	0.3583 (2)	1.2675 (2)	0.5559 (2)	0.0358 (9)
C(9)	0.2814 (2)	0.6219 (2)	0.6493 (2)	0.0398 (8)	C(21)	0.3327 (2)	1.1763 (2)	0.5068 (2)	0.0329 (7)
C(10)	0.2896 (2)	0.7208 (2)	0.6370 (2)	0.0306 (7)	Cl(1)	0.45898 (4)	1.17677 (6)	0.85386 (5)	0.0395 (2)
C(11)	0.2427 (2)	0.8018 (2)	0.6301 (2)	0.0300 (8)	Cl(2)	0.28390 (5)	1.17562 (8)	0.37652 (6)	0.0483 (3)
C(12)	0.1821 (2)	0.7901 (3)	0.6322 (2)	0.0381 (9)	O(w)	0.0100 (1)	1.0567 (2)	0.3965 (2)	0.0610 (8)
				$[Cu_2(terpy)_2(CA)](PF_6)_2$					
Cu	0.50118 (7)	0.41024 (5)	0.72855 (4)	0.0341 (5)	C(15)	0.5581 (8)	0.6403 (5)	0.7638 (4)	0.053 (7)
N(1)	0.4918 (5)	0.2543 (4)	0.7151 (2)	0.038 (4)	O(1)	0.3402 (4)	0.4658 (3)	0.6153 (2)	0.038 (3)
N(2)	0.4001 (5)	0.3734 (4)	0.8156 (2)	0.037 (4)	O(2)	0.6319 (4)	0.4387 (3)	0.6530 (3)	0.037 (3)
N(3)	0.5007 (5)	0.5507 (3)	0.7843 (2)	0.037 (4)	C(16)	0.4089 (5)	0.4828 (4)	0.5595 (3)	0.029 (4)
C(1)	0.5500 (8)	0.1969 (6)	0.6626 (4)	0.053 (7)	C(17)	0.5775 (5)	0.4676 (4)	0.5805 (3)	0.031 (4)
C(2)	0.5481 (9)	0.0893 (7)	0.6640 (5)	0.066 (9)	C(18)	0.6583 (5)	0.4837 (4)	0.5201 (3)	0.029 (4)
C(3)	0.4851 (9)	0.0394 (6)	0.7204 (6)	0.065 (9)	Cl(1)	0.8479 (1)	0.4692 (1)	0.54287 (8)	0.044 (1)
C(4)	0.4226 (9)	0.0965 (6)	0.7739 (5)	0.059 (8)	P(1)	0.8215 (2)	0.3003 (1)	0.9219 (1)	0.044 (1)
C(5)	0.4262 (6)	0.2041 (5)	0.7706 (3)	0.042 (5)	F(1)	0.9563 (8)	0.2284 (8)	0.9154 (6)	0.08 (1)
C(6)	0.3712 (6)	0.2737 (5)	0.8274 (3)	0.041 (5)	F(2)	0.687 (1)	0.3686 (9)	0.9322 (7)	0.08 (1)
C(7)	0.3038 (7)	0.2447 (6)	0.8911 (4)	0.053 (7)	F(3)	0.2736 (6)	0.7898 (4)	0.1250 (3)	0.090 (7)
C(8)	0.2704 (8)	0.3218 (7)	0.9419 (4)	0.059 (9)	F(4)	0.0807 (7)	0.6108 (4)	0.0316 (3)	0.099 (8)
C(9)	0.3041 (7)	0.4249 (6)	0.9308 (4)	0.050 (7)	F(5)	0.1764 (9)	0.7507 (7)	0.9910 (5)	0.074 (9)
C(10)	0.3716 (6)	0.4488 (5)	0.8652 (3)	0.041 (5)	F(6)	0.185 (1)	0.6519 (6)	0.1642 (4)	0.08 (1)
C(11)	0.4234 (6)	0.5524 (5)	0.8457 (3)	0.038 (5)	F(7)	0.051 (3)	0.672 (4)	0.123 (3)	0.08 (4)
C(12)	0.3995 (8)	0.6432 (6)	0.8850 (4)	0.054 (7)	F(8)	0.317 (5)	0.721 (4)	0.049 (2)	0.10 (6)
C(13)	0.4566 (9)	0.7351 (7)	0.8629 (5)	0.068 (9)	F(9)	0.272 (5)	0.615 (3)	0.137 (3)	0.10 (7)
C(14)	0.5388 (9)	0.7325 (6)	0.8032 (5)	0.065 (9)	F(10)	0.071 (7)	0.772 (2)	0.029 (3)	0.07 (8)

[a] Anisotropically refined atoms are given in the form of the isotropic equivalent thermal parameter defined as $U_{eq} = (U_{11}U_{22}U_{33})^{1/3}$.

of I and III are listed all together in order to facilitate their comparison.

The interatomic bond distances and angles of the ligands are similar to those found in other related compounds.[9,14,21-25] The planarity of the terpy ligand, as well as its rigidity (bite value around 1.28), is once again confirmed. However, both the conformation and coordination modes of the CA ligand differ significantly in compounds I and III. In the former, the CA dianion acts as a bidentate terminal ligand, whereas in the latter, it bridges two copper ions in a bis-bidentate fashion. So, whereas in I, C–O bonds of equal length are located in ortho positions, in III they are in para positions. The different conformations can be understood by taking into account that C–O lengths are related to the bond interactions of the oxygen atoms with the surrounding atoms. The shortest C–O bonds correspond in I to the oxygen atoms linked to the water molecules (O(3) and O(4); d(C–O) = 1.229 (2) Å) and in III to the O(1) oxygen atom (d(C–O) = 1.245 (6) Å), which shows the longest copper to oxygen bond length (d(Cu–O) = 2.268 (3) Å). The longest C–O bonds are associated in I with the Cu–O bonds (d(Cu–O) = 2.048 (7) Å, d(C–O) = 1.270 (3) Å) and in III with the strongest Cu–O bonds (d(C–O) = 1.266 (5) Å, d(Cu–O) = 1.943 (4) Å).

The geometry around the copper ion in both compounds may be viewed as intermediate between trigonal bipyramidal (TBP) and square pyramidal (SP). The main differences between these coordination geometries (see Table II and Figures 2 and 3) concern Cu–O distances and O(2)–Cu–N(2) and O(1)–Cu–N(2) angles. Thus, whereas in the monomer Cu–O bond distances are almost equal, in the dimer CA chelates to each copper(II) ion unsymmetrically. This latter coordination mode is usually found in dimeric or polymeric CA complexes.[9] When the longer Cu–O distance is viewed as the apical direction of a square pyramid, the remaining oxygen atom and the three nitrogen atoms define the basal plane. In both compounds the N(1)–Cu–N(3) angle is close (ca. 160°) in agreement with the rigidity imposed by the terpy ligand. Then, the distortion from SP can be related to the O(2)–Cu–N(2) and O(1)–Cu–N(2) angles. For compound III, these angles (170.6 (1) and 111.5 (1)°) are close to those shown by a SP geometry (180 and 90°), while in I these (143.42 (9) and 136.82 (9)°) agree better with a TBP geometry (120°). Moreover, in III the basal atoms (N(1), N(2), N(3), and O(2)) are practically coplanar within ±0.005 Å and the copper atom is displaced 0.160 (1) Å above this plane, while in I the least-squares plane through the basal atoms (N(1), N(2), N(3), and O(1)) is apart from them (within ±0.29 Å) and from the copper atom (0.38 Å).

For each coordination sphere of the copper atom a study of the distortion from ideal shapes is reported in Table IV. All the following caculations have been made by using the polyhedra resulting from projecting the coordinated atoms onto a sphere of unit radius centered on the copper atom.[26]

The method of Muetterties[27] using the analytical formula proposed by Galy[28] leads to a rate of distortion from the TBP to the SP geometry of 0.49 for I and 1.09 for III. Results obtained

(21) Goldschmied, E.; Stephenson, N. C. *Acta Crystallogr. Sect. B: Struct. Crystallogr. Cryst. Chem.* **1970**, *B26*, 1867.
(22) Savariault, J. M.; Rojo, T.; Arriortua, M. I.; Galy, J. *C. R. Acad. Sci., Ser. 2* **1983**, *(II)297*, 895.
(23) Allmann, R.; Kremer, S.; Kucharzcyk, D. *Inorg. Chim. Acta* **1984**, *L19*, 85.
(24) Henke, W.; Kremer, S.; Reinen, D. *Inorg. Chem.* **1983**, *22*, 2858.
(25) Kepert, D. L.; Kucharski, E. S.; White, A. H. *J. Chem. Soc., Dalton Trans.* **1980**, 1932.
(26) Kouba, J. K.; Wreford, S. S. *Inorg. Chem.* **1976**, *15*, 1463.
(27) Muetterties, E. L.; Guggenberger, L. J. *J. Am. Chem. Soc.* **1974**, *96*, 1748.
(28) Galy, J.; Bonnet, J. J.; Anderson, S. *Acta Chem. Scand., Ser. A* **1979**, *A33*, 383.

Table III. Interatomic Distances (Å) and Angles (deg)

	I	III		I	III
		Copper Coordination Sphere			
Cu–O(1)	2.041 (2)	2.268 (2)	Cu–N(2)	1.931 (3)	1.932 (3)
Cu–O(2)	2.054 (2)	1.943 (2)	Cu–N(3)	2.027 (3)	2.029 (3)
Cu–N(1)	2.019 (3)	2.017 (3)			
O(1)–Cu–O(2)	79.71 (8)	77.9 (1)	O(2)–Cu–N(2)	136.82 (9)	170.6 (1)
O(1)–Cu–N(1)	98.7 (1)	102.4 (1)	O(2)–Cu–N(3)	96.4 (1)	100.8 (2)
O(1)–Cu–N(2)	143.42 (9)	111.5 (1)	N(1)–Cu–N(2)	80.1 (1)	79.8 (2)
O(1)–Cu–N(3)	96.6 (1)	92.2 (1)	N(1)–Cu–N(3)	160.0 (1)	158.5 (1)
O(2)–Cu–N(1)	98.9 (1)	97.6 (2)	N(2)–Cu–N(3)	80.0 (1)	80.2 (2)
		Average Values in the Terpyridine Moiety			
C–N	1.345 (4)	1.343 (7)	C–C(intercycle)	1.478 (5)	1.468 (8)
C–C(intracycle)	1.378 (5)	1.377 (10)	C–H	0.90 (3)	0.90 (8)
C–C–C(intracycle)	119.2 (3)	119.3 (5)	C–C–N(intercycle)	113.2 (3)	113.5 (6)
C–C–C(intercycle)	125.8 (3)	125.6 (6)	C–N–C	119.7 (3)	119.6 (5)
C–C–N(intracycle)	121.4 (3)	121.1 (6)			
		Chloranilate Moiety			
C(16)–C(17)	1.531 (4)	1.536 (7)	C(16)–O(1)	1.273 (4)	1.245 (6)
C(17)–C(18)	1.376 (4)	1.381 (7)	C(17)–O(2)	1.268 (4)	1.266 (5)
C(18)–C(19)	1.421 (4)	1.411 (6)	C(18)–Cl(1)	1.741 (4)	1.723 (5)
C(19)–C(20)	1.548 (4)		C(19)–O(3)	1.227 (4)	
C(20)–C(21)	1.417 (4)		C(20)–O(4)	1.231 (4)	
C(21)–C(16)	1.375 (4)		C(21)–Cl(2)	1.736 (3)	
C(16)–C(17)–C(18)	119.6 (3)	119.0 (4)	O(2)–C(17)–C(18)	124.9 (3)	124.1 (4)
C(17)–C(18)–C(19)	122.6 (3)	121.9 (4)	Cl(1)–C(18)–C(17)	118.5 (2)	119.7 (3)
C(18)–C(19)–C(20)	122.6 (3)		Cl(1)–C(18)–C(19)	118.8 (2)	118.3 (4)
C(19)–C(20)–C(21)	118.4 (3)		O(3)–C(19)–C(18)	125.2 (3)	
C(20)–C(21)–C(16)	117.5 (3)		O(3)–C(19)–C(20)	117.3 (3)	
C(21)–C(16)–C(17)	119.1 (3)	119.0 (4)	O(4)–C(20)–C(19)	117.1 (3)	
O(1)–C(16)–C(17)	115.5 (2)	116.2 (4)	O(4)–C(20)–C(21)	124.5 (3)	
O(1)–C(16)–C(21)	125.4 (3)	124.7 (4)	Cl(2)–C(21)–C(16)	119.3 (2)	
O(2)–C(17)–C(16)	115.5 (2)	116.8 (4)	Cl(2)–C(21)–C(20)	118.1 (2)	
		Average Distance in PF_6 Ion			
P–F		1.548 (8)			
		Water Molecule			
O(w)–H(1w)	0.78 (5)		O(w)···O′(3)[a]	2.836 (3)	
O(w)–H(2w)	0.88 (5)		O(w)···O(4)	2.971 (4)	
O(w)···O(3)	3.137 (4)				
H(1w)–O(w)–H(2w)	105 (5)		O(w)–H(1w)–O′(3)	170 (4)	
O(4)–O(w)–O(3)	51.8 (2)		O(w)–H(2w)–O(4)	179 (3)	
O(4)–O(w)–O′(3)	110.2 (1)				

[a] O′(3) from O(3) by a translation of $^1/_2 + x$, $^1/_2 - y$, $^1/_2 + z$.

from other calculations such as the repulsion energy method proposed by Kepert[29] and the standard deviation of the angles around the copper atom point toward similar kinds of distortions (Table IV). The relatively dispersed numerical values show the difficulty in evaluating distortion effects when working with multidentate rigid ligands. In any event, all the above remarks allow us to conclude that although distortions are appreciable, the geometry of the coordination sphere around a copper atom is close to SP in III whereas these distortions shift toward TPB in I.

Finally, it can be noted that in III PF_6^- is located opposite to the O(1) atom (Figure 4). The distance Cu–P is equal to 4.152 (4) Å, the distances Cu–F(6) (3.178 (8) Å) and Cu–F(9) (2.760 (9) Å) are relatively short, and the angles O(1)–Cu–F(6) and O(1)–Cu–F(9) are 156.22 (8) and 167.06 (6)°, respectively (the F(9) fluorine atom corresponds to the F(6) atom after a rotation of $\pi/8$ around the F(3)–F(4) axes). If we consider the possibility of interactions between PF_6^- and copper(II) ions, the environment of the latter would be described as a distorted octahedron. On such an assumption, a rate of distortion, in the Muetterties–Galy model, from the regular octahedron to the SP geometry of 0.73 can be evaluated.

Infrared and Electronic Spectra. IR spectra of the four reported complexes exhibit bands due to C–O stretching vibrations, in the range 1200–1700 cm^{-1}. These bands are in agreement with the CA symmetry present in complexes I–III. In I, the CA group has approximately C_{2v} symmetry, exhibiting bands at 1630 (m), 1540 (vs), and 1370 (m) cm^{-1}. The presence of carbonyl bands above 1600 cm^{-1} is associated with localized C=O groups,[9] in accord with structural results. In the dimers II and III the symmetry of the CA ligand is close to D_{2h} and only two C–O

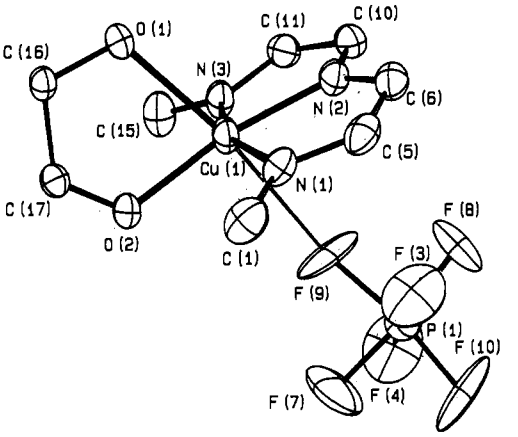

Figure 4. Detailed view of the coordination sphere of the copper atom in III. Only one orientation of the PF_6 anion is represented for clarity.

(29) Kepert, D. L. *J. Chem. Soc., Dalton Trans.* **1974**, 612.

Table IV. Rate of Distortion (Δ) of the Coordination Polyhedron around the Copper(II) Ion with Respect to the Ideal TBP and SP Geometries

Muetterties–Galy Method[a]

	dihedral angle, deg			
atoms	TBP	I	III	SP
O(a)–O(e)–N(1)–N(2)	101.5	95.3	117.5	119.8
O(a)–N(1)–N(2)–O(e)	101.5	129.8	135.2	119.8
O(a)–N(2)–N(3)–O(e)	101.5	129.0	131.8	119.8
O(a)–N(3)–O(e)–N(2)	101.5	94.7	109.9	119.8
N(1)–O(a)–O(e)–N(3)	53.1	87.4	89.9	75.7
N(1)–O(a)–N(2)–N(3)	53.1	35.2	55.9	75.7
N(2)–O(a)–N(1)–O(e)	101.5	90.6	70.2	75.7
N(2)–O(a)–N(3)–O(e)	101.5	90.2	77.5	75.7
N(1)–O(e)–N(2)–N(3)	53.1	28.5	0.1	0.0
Δ	0.0	0.49	1.09	1.0

Kepert Method[b]

	TBP	I	III	SP
θ, deg	180.0	176.7		129.0
$\sum 1/r_{ij}$, Å^{-1}	6.563	6.565		6.693
Δ	0.0	0.063		1.0
θ, deg	180.0		151.6	128.9
$\sum 1/r_{ij}$, Å^{-1}	6.574		6.615	6.696
Δ	0.0		0.590	1.0

Standard Deviations of Angles Method[c]

	TBP	I	III	SP
σ	27.49	27.53	30.64	36.00
Δ	0.0	0.05	0.58	1.00

[a] O(a) = apical oxygen atom, O(1) in III and O(2) in I; O(e) = equatorial oxygen atom, O(2) in III and O(1) in I. [b] θ = angle between the Cu–N(2) direction and the bisectrix of the O(1)–Cu–O(2) angles. The difference for the SP values between I and III corresponds to the discrepancy of the O(1)–Cu–O(2) angles. r_{ij} = distance between atoms i and j; i, j = O(1), O(2), N(1), N(2), and N(3). [c] $\sigma = [\sum(A_{ij} - A_{av})^2/(n-1)]^{1/2}$; A_{ij} = angle i–Cu–j; $A_{av} = A_{ij}/n$; n = number of A_{ij} angles.

stretching bands are observed in the IR spectra at 1520 (vs) and 1380 (m) cm^{-1}. Further, the spectrum of I shows a sharp band of medium intensity at 3480 cm^{-1} (with a shoulder at 3500 cm^{-1}) assignable to the O–H stretching vibrations of hydrogen-bonded, not clustered, water molecules.[30] In the oxalate complex IV, which was not structurally characterized, the number of bands agrees with C_{2v} or D_{2h} symmetry for this anion. Nevertheless, the positions of these bands (1625 (vs) and 1290 (m) cm^{-1}) suggest a bridging bis-bidentate coordination mode,[31] thus supporting the dimeric arrangement proposed for this complex.

Electronic spectra consist of broad bands in all cases. Spectra of CA complexes are dominated by "forbidden" internal charge-transfer bands (the compounds are purple) arising from this dianion.[32] For I, the CT band is observed around 18 000 cm^{-1}, in agreement with the *o*-benzoquinone character of CA in this complex, whereas for II and III this appears above 22 000 cm^{-1}, as expected for *p*-benzoquinones.[32] Then, in I the overlapping of the CT band makes it difficult to locate the d–d copper(II) bands. In the spectra of II and III, the shift of this band to higher energies allows one easily to observe a broad d–d band with two relative maxima centered at about 14 000 and 17 000 cm^{-1}, in agreement with the geometry found around the copper(II) ion.[33,34] On the other hand, electronic spectra of IV exhibit one unresolved broad band with a maximum centered around 15 000 cm^{-1} consistent with a copper coordination sphere of near distorted SP geometry.[33,34]

Table V. EPR and Magnetic Parameters of the Studied Complexes

compd	$g_\parallel$[a]	$g_\perp$[a]	other features[b]	J, cm^{-1}
I	2.23	2.06	$\Delta M_s = 2$ S–T	0.10–0.12[c]
II	2.22 (2.23, 2.07, 2.05)	2.06	$\Delta M_s = 2$ S–T	0.05–0.07[c]
III	2.22 (2.23, 2.07, 2.05)	2.06	$\Delta M_s = 2$ S–T	0.04–0.05[c]
IV	2.23	2.05	$\Delta M_s = 2$	–0.8

[a] X-Band EPR spectra *g* values. Data from Q-band are given in parentheses. [b] S–T = singlet-to-triplet transitions. [c] Absolute values obtained from S–T transitions.

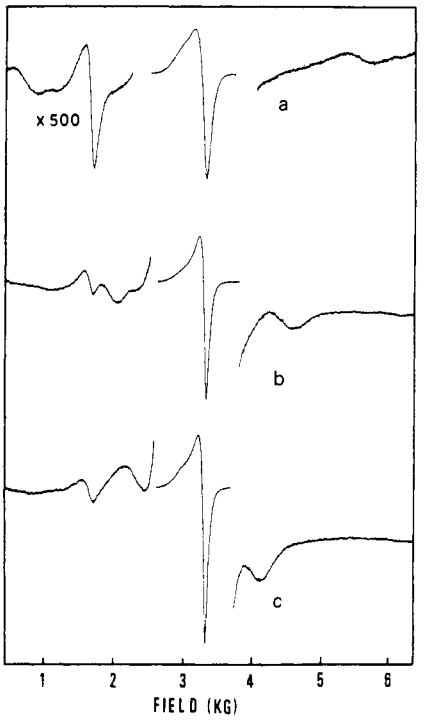

Figure 5. X-Band EPR spectra of (a) complex I (100 K), (b) complex II (400 K), and (c) complex III (400 K). The spectrometer gain of low- and high-field portions of the spectra is multiplied by 500.

Magnetic Behavior and EPR Spectra. From 298 down to 4.2 K the μ_{eff} values of compounds I–III stay practically constant ($\mu_{eff} = 1.9\ \mu_B$). Thus, no exchange interactions are detectable for these compounds through the susceptibility data, indicating that $|J| < 0.5$ cm^{-1}. For the oxalate compound μ_{eff} varies from 1.86 at 298 K to 1.63 μ_B at 4.2 K. Magnetic data were least-squares-fit to the Bleaney–Bowers equation[35] for isotropic exchange in a $S = {}^1/_2$ dimeric system. When the *g* value at 2.11 is fixed (from EPR measurements), a singlet ground state results from this fit at 1.6 cm^{-1} ($-2J$) below the triplet state.

EPR results are reported in Table V. X-Band EPR spectra show very similar axial signals for all complexes, with a perpendicular component at g = ca. 2.06 and a shoulder derivative around 2.23 (this signal can be better resolved in the Q-band spectra, and for complexes II and III three *g* values are detected).

Besides this large signal, which corresponds to the $\Delta M_s = \pm 1$ allowed transitions, the complexes exhibit weak-intensity features in their X-band spectra. All complexes show a feature at ca. 1650 G corresponding to the $\Delta M_s = \pm 2$ forbidden transition, which indicates a magnetic coupling between two Cu(II) ions.

Furthermore, two weak signals located at lower and higher field values of the normal $\Delta M_s = \pm 1$ transition are seen in the three chloranilate compounds (Figure 5). These can be assigned as forbidden transitions between the singlet electronic state of an

(30) Falk, M.; Knop, O. In *Water: a Comprehensive Treatise*; Frank, F., Ed.; Plenum: New York, 1973; Vol. 2, Chapter 2.
(31) Nakao, Y.; Yamazaki, M.; Suzuki, S.; Mori, W.; Nakahara, A.; Matsumoto, K.; Ooi, S. *Inorg. Chim. Acta* **1983**, *74*, 159.
(32) Morton, R. A. In *Biochemistry of Quinones*; Morton, R. A., Ed.; Academic: London, 1965; Chapter 2.
(33) Hathaway, B. J. *Coord. Chem. Rev.* **1982**, *41*, 423. Hathaway, B. J. *Struct. Bonding (Berlin)* **1984**, *57*, 55 and references therein.
(34) Lever, A. B. P. *Inorganic Electronic Spectroscopy*, 2nd ed.; Elsevier: Amsterdam, 1985; p 568.
(35) Bleaney, B.; Bowers, K. D. *Proc. R. Soc. London, Ser. A* **1952**, *214*, 451.

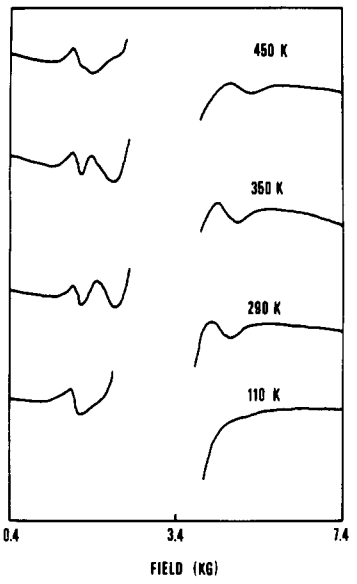

Figure 6. Variation of low- and high-field X-band EPR spectra of complex II with temperature.

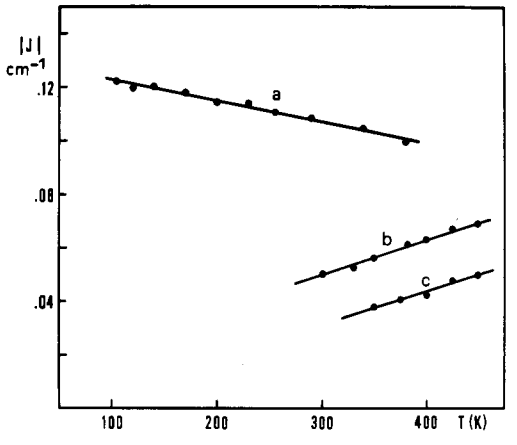

Figure 7. Temperature dependence of $|J|$ of (a) complex I, (b) complex II, and (c) complex III.

exchange-coupled copper(II) dimer and the $M_s = \pm 1$ components of the triplet state.[10] We observed that while signals associated with the triplet $\Delta M_s = \pm 1$ and $\Delta M_s = \pm 2$ transitions remain nearly unchanged in the range of temperatures 100–500 K, a pronounced shift with temperature is detected for the two singlet–triplet transitions (Figure 6). When it is taken into account that each of these transitions is located at $2|J|/g\beta$ to either higher or lower field of the allowed transition, $|J|$ variation with the temperature can be calculated for the three chloranilate compounds as illustrated in Figure 7. The same temperature dependence of $|J|$ is observed for the isostructural complexes II and III: a significant linear decrease of $|J|$ (about 40%) between 450 and 300 K. This evolution is somewhat different for complex I, which shows a weak linear increase of $|J|$ (about 20%) when the temperature decreases from 400 to 100 K.

It has been suggested that changes in $|J|$ values with temperature arise, for weakly coupled cases, from lattice shrinkage effects.[10] Then, it is not surprising, owing to the two very different molecular arrangements exhibited by these complexes, to have distinct thermal dependences of $|J|$. Hence, the close dependence of $|J|$ on temperature for complexes II and III suggests that dimensional changes within the dimeric entity $[Cu_2(terpy)_2(CA)]^{2+}$ are at the origin of the observed trend, being independent of the counterion nature. Expressing J as sum of temperature-independent (J_0) and -dependent terms ($J(T)$), it is to be expected that $J(T)$ gives an estimate of the lattice effects in similar molecular entities. Then, the pronounced relative variation of J actually arises from the small magnitude of J_0, which here becomes comparable to $J(T)$.

Magnetic Exchange Mechanisms. In contrast to the case for complexes II–IV, where the exchange is clearly propagated through CA or OX ligands, respectively, the unusual "pseudo-dimeric" arrangement found in I could involve three potential interaction pathways: (i) a "through space" dipolar path, (ii) a superexchange path via an overlap between two terpy rings of adjacent Cu(terpy)CA moieties, and (iii) a superexchange "complex" path through a very extended bridging network formed by two CA and two water molecules connected by hydrogen bonds. Let us briefly discuss these possibilities. When it is taken into account that the intradimeric Cu–Cu distance is 5.648 Å, a direct dipolar interaction, which is known to vary as r^{-3}, r being the interspin distance, can be assumed to be negligible ($<10^{-2}$ cm^{-1}). This conclusion is also supported by the appearance of a half-field EPR signal. In our case, since the intra- and interdimeric Cu–Cu distances are nearly equal, this observation indicates that the interactions in the pairs are much more important than interactions between pairs (which are purely dipolar).

The second path involves a "quasi-direct" interaction through two parallel terpy ligands, which are separated by 3.63 Å in such a way that a N–C side of a pyridine (py) ring is positioned directly over another N′–C′ side of the adjacent ring (see Figure 1). Then, the exchange occurs through a py–py bridging network. In fact, ab initio MO calculations on the py–py network show that the HOMO's (lying at −0.29 au) are of π type with large contributions from the p_z carbon orbitals. Such MO's are quite inadequate to overlap with the metal magnetic orbitals that are directed toward the σ nitrogen orbitals. In any event, the higher MO's of the σ type do not lie too far in energy from the HOMO's (ca. −0.33 au) and could prove suitable to propagate the exchange.

The alternative superexchange path seems, a priori, to be reasonable, given the ability of CA and water molecules to support the exchange.[36] Nevertheless, the observed $|J|$ values are significantly higher than those expected for such a large exchange distance (estimated to be around 18 Å). Thus, Coffman and Buettner[37] proposed an experimentally determined function for long-range ferromagnetic and antiferromagnetic superexchange that establishes the limit of exchange interactions observed at any distance. According to this function, an interacting distance no longer than 9–10 Å was needed for the detected $|J|$ value. In other words, $|J|$ values less than 10^{-5}–10^{-6} cm^{-1} are expected for exchange distances of 17–18 Å. Such an observation supports the py–py path (trough ca. 8 Å) rather than the longer superexchange path of 18 Å, thus constituting indirect evidence about the exchange mechanism of compound I. In any event, this evidence cannot be taken as conclusive since several exceptions to the Coffman rule have been reported.[36]

Let us now compare the range of the exchange interactions observed in the reported complexes (Table V). In the case of the dimeric entities $[Cu_2(terpy)_2L]^{2+}$ (where L = OX, CA), the actual geometry of these ions[18] is unfavorable to transmit the exchange coupling. Thus, in the ideal case of assuming regular SP surroundings of each copper(II) ion, the coupling constant J becomes zero[38] since the magnetic orbitals, of $x^2 - y^2$ type, are essentially localized in the basal planes. In the reported complexes, as usually occurs, the surroundings of the copper(II) ion exhibit some TBP or octahedral character. Consequently, the magnetic orbitals acquire some z^2-type character, with a resultant delocalization on the apical site (z direction), which allows a weak coupling. Thus, the weaker interactions shown by chloranilate complexes (II, III) compared to that of the oxalate complex (IV) reflect the change of bridging ligand and arise from the greater interaction of the exchange-propagating orbitals of the oxalate, lying at higher energy, with the $d_{x^2-y^2}$ metal orbitals.[9] On the other hand, the difference in exchange interactions in the chloranilate complexes may be related to the ability of ClO_4 and PF_6 counterions to semicoordinate to the Cu(II) ions to give a pseudooctahedral

(36) See: Hendrickson, D. N. In ref 1, p 523, and references therein.
(37) Coffman, R. E.; Buettner, G. R. *J. Chem. Phys.* **1979**, *83*, 2387.
(38) Kahn, O.; Morgestern-Badarau, I.; Block, R. *Chem. Phys. Lett.* **1984**, *108*, 457.

environment. The semicoordination affects somewhat the energies of d orbitals, displacing, in particular, the d_{z^2} orbital to higher energies. As the ability of the counterion to coordinate becomes stronger, that is, as the size becomes smaller, d_{z^2} and $d_{x^2-y^2}$ orbitals approach each other in energy. Hence, an increase of a z^2-type contribution in the magnetic orbital, which could promote an increase in antiferromagnetic exchange interaction, would be expected. From the above argument, the stronger $|J|$ value exhibited by the ClO_4 complex (II) compared to the PF_6 one (III) could be in agreement with the smaller size of the former counterion, if a negative sign of J (antiferromagnetic coupling) is assumed.

Finally, the different temperature dependence of $|J|$ observed in Figure 7 could be suggestive of different signs of the values of J. In fact, preliminary EPR results on similar systems containing the BF_4^- counterion agree with a minimum in the plot of $|J|$ vs T.[39] This observation may be indicative of a reversal in the sign of J.[40] Further investigations on these and similar systems are still required in order to conclude about the sign of the exchange and are in progress.

Acknowledgment. This work was partially supported by the Comision Asesora de Investigacion en Ciencia y Tecnologia under Grant 2930/84. J.V.F. thanks the Spanish Ministerio de Educacion y Ciencia for a FPI fellowship.

Registry No. I, 111435-04-2; II, 111554-23-5; III, 111435-03-1; IV, 111433-86-4.

Supplementary Material Available: Tables SI-SVI, listing atomic coordinates, thermal parameters, hydrogen positions, bond distances and angles, and mean least-squares planes for I and III, and Table SIX, listing experimental and calculated magnetic susceptibility data for IV (15 pages); Tables SVII and SVIII, listing calculated and observed structure factors for I and III (33 pages). Ordering information is given on any current masthead page.

(39) Folgado, J. V. Ph.D. Thesis, University of Valencia, Valencia, Spain, 1987.

(40) Reibenspies, J. H.; Anderson, O. P.; Eaton, S. S.; More, K. M.; Eaton, G. R. *Inorg. Chem.* **1987**, *26*, 132.

Contribution from the Department of Chemistry and Laboratory for Molecular Structure and Bonding, Texas A&M University, College Station, Texas 77843

Syntheses and X-ray Structures of Group 11 Pyrazole and Pyrazolate Complexes. X-ray Crystal Structures of Bis(3,5-diphenylpyrazole)copper(II) Dibromide, Tris(μ-3,5-diphenylpyrazolato-*N*,*N*′)trisilver(I)-2-Tetrahydrofuran, Tris(μ-3,5-diphenylpyrazolato-*N*,*N*′)trigold(I), and Hexakis(μ-3,5-diphenylpyrazolato-*N*,*N*′)hexagold(I)

H. H. Murray,† Raphael G. Raptis,†‡ and John P. Fackler, Jr.*

Received June 15, 1987

The reaction of anhydrous $CuBr_2$ with 3,5-diphenylpyrazole in a 1:2 ratio in THF yields bis(3,5-diphenylpyrazole)dibromocopper(II). The reaction of $AgNO_3$ in THF with sodium 3,5-diphenylpyrazolate gives tris(μ-3,5-diphenylpyrazolato-*N*,*N*′)trisilver(I). The reaction of $Au(S(CH_2)_4)Cl$ with 1 molar equiv of sodium 3,5-diphenylpyrazolate in THF yields tris(μ-3,5-diphenylpyrazolato-*N*,*N*′)trigold(I). Hexakis(μ-3,5-diphenylpyrazolato-*N*,*N*′)hexagold(I) was obtained from a reaction of $Au(PPh_3)Cl$, AgO_2CPh, and sodium 3,5-diphenylpyrazolate in THF. The monomer, both trimers, and the hexamer have been characterized by X-ray crystallography. The copper monomer, bis(3,5-diphenylpyrazole)dibromocopper(II), crystallizes in the monoclinic space group $P2_1/n$ (No. 14) with cell dimensions of a = 14.644 (3) Å, b = 11.679 (2) Å, c = 16.640 (3) Å, β = 108.82 (2)°, V = 2693.6 (8) Å^3, and Z = 4. The four-coordinate Cu(II) center has a geometry best described as being between tetrahedral and square planar. The silver trimer, $[Ag(\mu\text{-}3,5\text{-}Ph_2pz)]_3 \cdot 2THF$,§ crystallizes in the monoclinic space group $P2_1/n$ (No. 14) with cell dimensions of a = 14.066 (6) Å, b = 14.987 (3) Å, c = 23.306 (6) Å, β = 106.88 (3)°, V = 4701 (3) Å^3, and Z = 4. The three silver centers are bridged by three 3,5-diphenylpyrazolate units. The Ag···Ag distances are significantly different (3.305 (2), 3.362 (2), and 3.486 (2) Å). The nine-membered Ag_3N_6 ring is not planar. The gold trimer, $[Au(\mu\text{-}3,5\text{-}Ph_2pz)]_3$, crystallizes in the trigonal space group $R\bar{3}c$ (No. 167) with cell dimensions (on hexagonal axes) of a = 16.091 (3) Å, c = 25.726 (4) Å, V = 5770 (2) Å^3, and Z = 6. The gold centers form an equilateral triangle with nonbonding Au···Au distances of 3.368 (1) Å, bridged by pyrazolate ligands, giving a rigorously planar nine-membered inorganic ring with Au-N-N as the repeat unit. The hexamer, $[Au(\mu\text{-}3,5\text{-}Ph_2pz)]_6$, crystallizes in the monoclinic space group $P2_1/n$ (No. 14) with cell dimensions of a = 16.048 (3) Å, b = 17.850 (3) Å, c = 29.663 (5) Å, β = 92.47 (1)°, V = 8489 (2) Å^3, and Z = 4. This complex contains an 18-membered inorganic ring in the shape of a two-bladed propeller. The geometry of the six gold centers is best described as an edge-sharing bitetrahedron. The intramolecular Au···Au distances range from 3.085 (2) to 6.010 (1) Å.

The chemistry of pyrazole and pyrazolate metal complexes is quite extensive.[1] Monomeric pyrazole and pyrazolate coordination complexes are well-known;[2] dimeric species often contain two bridging pyrazolate ligands and have shown a plethora[3] of fascinating reactions. The pyrazolate ligand is known to form an A-frame-like bridge with rhodium dppm, dam, and dapm dimers.[4] Polymeric metal complexes containing a single pyrazolate bridge

* To whom correspondence should be addressed.

† Synthesis.

‡ Crystallography.

§ Abbreviations used: pz = pyrazolate anion; 3,5-Ph_2pz = 3,5-diphenylpyrazolate anion; 3,5-Me_2pz = 3,5-dimethylpyrazolate anion; 3,5-Ph_2pzH = 3,5-diphenylpyrazole; dppm = bis(diphenylphosphino)methane; dppe = 1,2-bis(diphenylphosphino)ethane; dam = bis(diphenylarsino)methane; dapm = (diphenylarsino)(diphenylphosphino)methane; THF = tetrahydrofuran; THT = tetrahydrothiophene; pz(11) identifies a μ-3,5-diphenylpyrazolate ring (metal coordinated) by using the crystallographic numbering scheme of the carbon in the 4-position of that ring.

(1) (a) Trofimenko, S. *Chem. Rev.* **1972**, *72*, 497. (b) Trofimenko, S. *Prog. Inorg. Chem.* **1986**, *34*, 115-210.

(2) (a) Sullivan, B. P.; Salmon, D. J.; Meyer, T. J.; Peadin, J. *Inorg. Chem.* **1979**, *18*, 3369. (b) Coletta, F.; Eltore, R.; Gambaro, A. *J. Inorg. Nucl. Chem.* **1975**, *37*, 314. (c) Rettig, S. J.; Singbeil, D. L.; Storr, A.; Trotter, J. *Can. J. Chem.* **1978**, *56*, 2099.

(3) (a) Atwood, J. L.; Beveridge, K. A.; Bushnell, G. W.; Dixon, K. R.; Eadie, D. T.; Stobart, S. R.; Zaworotko, M. J. *Inorg. Chem.* **1984**, *23*, 4050. (b) Bushnell, G. W.; Stobart, S. R.; Vefghi, R.; Zaworotko, M. J. *J. Chem. Soc., Chem. Commun.* **1984**, 282. (c) Beveridge, K. A.; Bushnell, G. W.; Stobart, S. R.; Atwood, J. L.; Zaworotko, M. J. *Organometallics* **1983**, *2*, 1447. (d) Powell, J.; Kuksis, A.; Nyburg, S. C.; Ng, W. W. *Inorg. Chim. Acta* **1982**, *64*, L211. (e) Usón, R.; Oro, L. A.; Ciriano, M. A.; Carmona, D.; Tiripicchio, A.; Camellini, M. T. *J. Organomet. Chem.* **1982**, *224*, 69.

0020-1669/88/1327-0026$01.50/0